Molecular modeling of 1, 4-Phenylenediacetonitrile dye sensitizer for solar cells using quantum chemical calculations

A. Prakasam[1,*] and P. M. Anbarasan[2]

[1]Department of Physics, Pachaiyappa's college for Men, Kanchipuram, Tamilnadu- 631501, India.
[2]Centre for Nanoscience & Nanotechnology, Periyar University, Salem - 636 011, Tamil Nadu, India.

ABSTRACT

The geometries, electronic structures, polarizabilities, and hyperpolarizabilities of organic dye sensitizer 1,4-Phenylenediacetonitrile was studied based on ab initio HF and Density Functional Theory (DFT) using the hybrid functional B3LYP. Ultraviolet-visible (UV-Vis) spectrum was investigated by Time Dependent DFT (TDDFT). Features of the electronic absorption spectrum in the visible and near-UV regions were assigned based on TDDFT calculations. The absorption bands are assigned to $\pi \rightarrow \pi^*$ transitions. Calculated results suggest that the three excited states with the lowest excited energies in 1,4-Phenylenediacetonitrile is due to photo induced electron transfer processes. The interfacial electron transfer between semiconductor TiO_2 electrode and dye sensitizer 1,4-Phenylenediacetonitrile, is due to an electron injection process from excited dye to the semiconductor's conduction band. The role of cyanine and methyl group in 1,4-Phenylenediacetonitrile in geometries, electronic structures, and spectral properties were analyzed.

Introduction

Because of the depletion of fossil fuels, growing demand of energy, global warming and other environmental problems, the development of environmental friendly renewable energy technologies is an urgent task for our human being [1]. Among all the renewable energy technologies, the nanocrystalline dye-sensitized solar cell (DSSC) system, a kind of photovoltaic device that presented by O'Regan and Gratzel in 1991, has attracted a lot of attention because of the potential application for low-cost solar electricity [2–5]. The main parts of DSSC are mesoporous oxide semiconductor layers that composed of nanoparticles and monolayer of dye sensitizers that attached to the surface of the semiconductor nano-films [3]. The dye sensitizers play an important role in DSSC that have a significant influence on the photoelectric conversion and transport performance of electrode [6–9]. Up to now, two kinds of dye sensitizers, which are generally known as metal-organic complexes and metal-free organic dyes, were studied extensively. In metal-organic complexes, especially the noble metal ruthenium polypyridyl complexes, including N3 and black dye etc. that were presented by Gratzel et al., have proved to be the best dye sensitizers with overall energy conversion efficiency greater than 10% under air mass (AM) 1.5 irradiation [10–12]. However, the limited metal Ru will become a bottleneck of application if the DSSC is widely used in our daily living [13]. On the other hand, metal-free organic dyes as sensitizers for DSSC, including cyanines, hemicyanines, triphenylmethanes, perylenes, coumarins, porphyrins, squaraines, indoline, and azulene- based dyes etc., have also been developed because of their high molar absorption coefficient, relatively simple synthesis procedure, various structures and lower cost [14–16]. In contrast to the numerous experimental studies of dye sensitizers, the theoretical investigations are relatively limited. Only several groups focused on the electronic structures and absorption properties of dye sensitizers [17–26], and Ru-complexes and organic dyes coupled TiO2 nanocrystalline [27–30], as well as the electron transfer dynamics of the interface between dyes and nanocrystalline [31–35]. Until now, it remains a severe challenge for both experiment and theory to elucidate the fundamental properties of the ultrafast electron injection [30], and to approach the satisfied efficiency of DSSC. Further developments in dye design will play a crucial part in the ongoing optimization of DSSC [36], and it depends on the quantitative knowledge of dye sensitizer. So the theoretical investigations of the physical properties of dye sensitizers are very important in order to disclose the relationship among the performance, structures and the properties, it is also helpful to design and synthesis novel dye sensitizers with higher performance. Recently a rapid progress of organic dyes has been witnessed reaching close to 10.0% efficiencies in combination with a volatile acetonitrile-based electrolyte [37]. Nitrile is an important class of high performance dyes, which are easily processable, and display good mechanical properties, outstanding thermal and thermal-oxidative stability. Nitrile dyes were used for aerospace, marine, and electronic packaging applications by thermal treatment of nitrile derivatives at elevated temperatures (generally high up to 350 °C) for an extended period of time. In this paper the performance of 1,4-Phenylenediacetonitrile metal free dye that can be used in DSSC is analyzed.

Computational methods

The computations of the geometries, electronic structures, polarizabilities and hyperpolarizabilities, as well as electronic absorption spectrum for dye sensitizer 1,4-Phenylenediacetonitrile was done using ab initio HF and DFT with Gaussian03 package [38]. The DFT was treated according to Becke's three parameter gradient-corrected exchange

potential and the Lee-Yang-Parr gradient-corrected correlation potential (B3LYP) [39–41], and all calculations were performed without any symmetry constraints by using polarized split-valence 6-311G(d,p) basis sets. The electronic absorption spectrum requires calculation of the allowed excitations and oscillator strengths. These calculations were done using TDDFT with the same basis sets and exchange-correlation functional in vacuum and solution, and the non-equilibrium version of the polarizable continuum model (PCM) [42,43] was adopted for calculating the solvent effects

Results and discussion

The geometric structure

The optimized geometry of the 1,4-Phenylenediacetonitrile is shown in Fig.1, and the bond lengths, bond angles and dihedral angles are listed in Table 1. Since the crystal structure of the exact title compound is not available till now, the optimized structure can be only be compared with other similar systems for which the crystal structures have been solved. From the theoretical values we can find that most of the optimized bond lengths, bond angles and dihedral angles. The distance between C2 - C3 and C3-C4 atoms in cyanine groups of 1,4-Phenylenediacetonitrile are 1.3972 and 1.3868 Å respectively at B3LYP/6-311++G (d,p) and also well matched with HF/6-311++G (d,p).
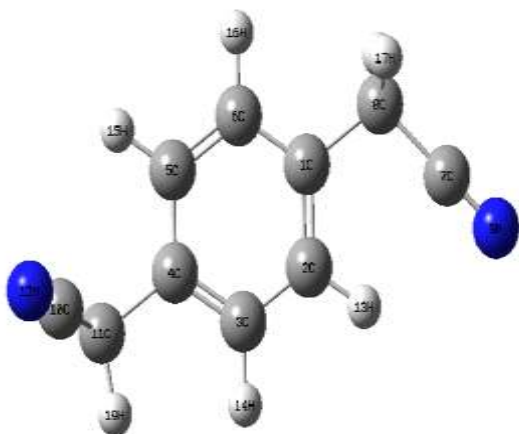

Figure 1. Optimized Geometrical Structure of Dye 1,4-Phenylenediacetonitrile

Electronic structures and charges

Natural Bond Orbital (NBO) analysis was performed in order to analyze the charge populations of the dye 1,4-Phenylenediacetonitrile. Charge distributions in C, N and H atoms were observed because of the different electro-negativity, the electrons transferred from C atoms to C, N atoms, C atoms to H. The natural charges of different groups are the sum of every atomic natural charge in the group. These data indicate that the cyanine and amide groups are acceptors, while the acetic groups are donors, and the charges were transferred through chemical bonds. The frontier molecular orbitals (MO) energies and corresponding density of state of the dye 1,4-Phenylenediacetonitrile is shown in Fig. 2. The HOMO–LUMO gap of the dye 1,4-Phenylenediacetonitrile in vacuum is 5.35 eV.

While the calculated HOMO and LUMO energies of the bare Ti$_{38}$O$_{76}$ cluster as a model for nanocrystalline are -6.55 and -2.77eV, respectively, resulting in a HOMO–LUMO gap of 3.78 eV, the lowest transition is reduced to 3.20 eV according to TDDFT, and this value is slightly smaller than typical band gap of TiO$_2$ nanoparticles with nm size [44]. Furthermore, the

HOMO, LUMO and HOMO–LUMO gap of (TiO$_2$)$_{60}$ cluster is -7.52, -2.97, and 4.55 eV (B3LYP/VDZ), respectively [45]. Taking into account of the cluster size effects and the calculated HOMO, LUMO, HOMO–LUMO gap of the dye 1,4-Phenylenediacetonitrile, Ti$_{38}$O$_{76}$ and (TiO$_2$)$_{60}$ clusters, we can find that the HOMO energies of these dyes fall within the TiO$_2$ gap.
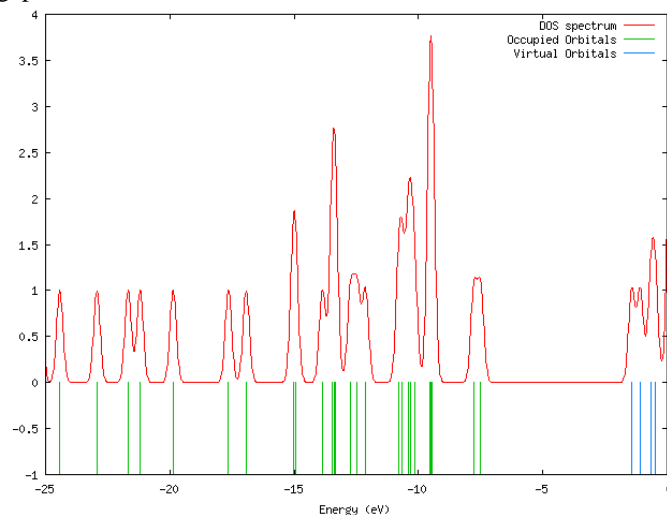

Figure 2. The frontier molecular orbital energies and corresponding density of state (DOS) spectrum of the dye 1,4-Phenylenediacetonitrile

The above data also reveal the interfacial electron transfer between semiconductor TiO$_2$ electrode and the dye sensitizer 1,4-Phenylenediacetonitrile is electron injection processes from excited dye to the semiconductor conduction band. This is a kind of typical interfacial electron transfer reaction [46].

Polarizability and hyperpolarizability

Polarizabilities and hyperpolarizabilities characterize the response of a system in an applied electric field [47]. They determine not only the strength of molecular interactions (long-range intermolecular induction, dispersion forces, etc.) as well as the cross sections of different scattering and collision processes, but also the nonlinear optical properties (NLO) of the system [48, 49]. It has been found that the dye sensitizer hemicyanine system, which has high NLO property, usually possesses high photoelectric conversion performance [50]. In order to investigate the relationships among photocurrent generation, molecular structures and NLO, the polarizabilities and hyperpolarizabilities of 1,4-Phenylenediacetonitrile was calculated.

The polarizabilities and hyperpolarizabilities could be computed via finite field (FF) method, sum-over state (SOS) method based on TD-DFT, and coupled-perturbed HF (CPHF) method. However, the use of FF, SOS, and CPHF methods with large sized basis sets for 1,4-Phenylenediacetonitrile is too expensive. Here, the polarizability and the first hyperpolarizabilities are computed as a numerical derivative of the dipole moment using B3LYP/6-31G(d,p). The definitions [48,49] for the isotropic polarizability is

$$\alpha = \frac{1}{3}\left(\alpha_{XX} + \alpha_{YY} + \alpha_{ZZ}\right)$$

The polarizability anisotropy invariant is

$$\Delta\alpha = \left[\frac{\left(\alpha_{XX} - \alpha_{YY}\right)^2 + \left(\alpha_{YY} - \alpha_{ZZ}\right)^2 + \left(\alpha_{ZZ} - \alpha_{XX}\right)^2}{2}\right]^{\frac{1}{2}}$$

and the average hyperpolarizability is

$$\beta_{\mathrm{P}} = \frac{1}{5}\left(\beta_{iiZ} + \beta_{iZi} + \beta_{Zii}\right)$$

Where, α_{XX}, α_{YY}, and α_{ZZ} are tensor components of polarizability; β_{iiZ}, β_{iZi}, and β_{Zii} (i from X to Z) are tensor components of hyperpolarizability.

Tables 2 and 3 list the values of the polarizabilities and hyperpolarizabilities of the dye 1,4-Phenylenediacetonitrile. In addition to the individual tensor components of the polarizabilties and the first hyperpolarizabilities, the isotropic polarizability, polarizability anisotropy invariant and hyperpolarizability are also calculated. The calculated isotropic polarizability of 1,4-Phenylenediacetonitrile is 81.03 a.u. However, the calculated isotropic polarizability of JK16, JK17, dye 1, dye 2, D5, DST and DSS is 759.9, 1015.5, 694.7, 785.7, 510.6, 611.2 and 802.9 a.u., respectively [51,52]. The above data indicate that the donor-conjugate p bridge-acceptor (D-p-A) chain-like dyes have stronger response for external electric field. Whereas, for dye sensitizers D5, DST, DSS, JK16, JK17, dye 1 and dye 2, on the basis of the published photo-to-current conversion efficiencies, the similarity and the difference of geometries, and the calculated isotropic polarizabilities, it is found that the longer the length of the conjugate bridge in similar dyes, the larger the polarizability of the dye molecule, and the lower the photo-to-current conversion efficiency. This may be due to the fact that the longer conjugate-p-bridge enlarged the delocalization of electrons, thus it enhanced the response of the external field, but the enlarged delocalization may be not favorable to generate charge separated state effectively. So it induces the lower photo-to-current conversion efficiency.

Electronic absorption spectra and sensitized mechanism

In order to understand the electronic transitions of 1,4-Phenylenediacetonitrile, TD-DFT calculations on electronic absorption spectra in vacuum and solvent were performed, and the results are shown in Fig. 3. It is observed that, for 1,4-Phenylenediacetonitrile, the absorption in the visible region is much weaker than that in the UV region. The calculated results have a red-shift. The results of TD-DFT have an appreciable red-shift, and the degree of red-shift in solvent is more significant than that in vacuum. The discrepancy between vacuum and solvent effects in TD-DFT calculations may result from two aspects. The first aspect is smaller gap of materials which induces smaller excited energies. The other is solvent effects. Measurements of electronic absorptions are usually performed in Solvent, especially polar solvent, could affect the geometry and electronic structure as well as the properties of molecules through the long-range interaction between solute molecule and solvent molecule. For these reasons it is more difficult to make the TD-DFT calculation is consistent with quantitatively. Though the discrepancy exists, the TD-DFT calculations are capable of describing the spectral features of 1,4-Phenylenediacetonitrile because of the agreement of lineshape and relative strength as compared with the vacuum and solvent.

The HOMO-LUMO gap of 1,4-Phenylenediacetonitrile in acetonitrile at B3LYP/6-31G (d,p) theory level is smaller than that in vacuum. This fact indicates that the solvent effects stabilize the frontier orbitals of 1,4-Phenylenediacetonitrile. So it induces the smaller intensities and red-shift of the absorption as compared with that in vacuum.

In order to obtain the microscopic information about the electronic transitions, the corresponding MO properties are checked. The absorption in visible and near-UV region is the

most important region for photo-to-current conversion, so only the 20 lowest singlet/singlet transitions of the absorption band in visible and near-UV region for 1,4-Phenylenediacetonitrile is listed in Table 4. The data of Table 4 and Fig. 4 are based on the 6-311G (d,p) results with solvent effects involved.
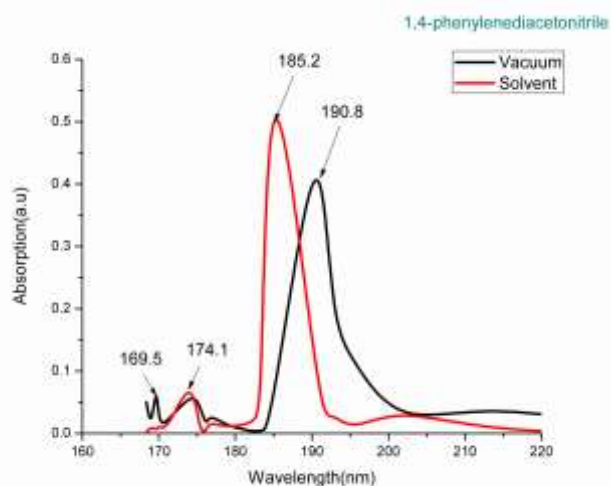

Figure 3. Calculated electronic absorption spectra of the dye 1,4-Phenylenediacetonitrile

This indicates that the transitions are photo induced charge transfer processes, thus the excitations generate charge separated states, which should favour the electron injection from the excited dye to semiconductor surface.

The solar energy to electricity conversion efficiency (η) under AM 1.5 white-light irradiation can be obtained from the following formula:

$$\eta(\%) = \frac{J_{SC}[mAcm^{-2}]V_{OC}[V]ff}{I_0[mWcm^{-2}]} \times 100$$

HOMO-3		LUMO+3	
	8.99		0.99
HOMO-2		LUMO+2	
	8.24		1.97
HOMO-1		LUMO+1	
	8.01		2.29
HOMO		LUMO	
	7.80		2.45

Figure .4. Isodensity plots (isodensity contour = 0.02 a.u.) of the frontier orbitals of 1,4-Phenylenediacetonitrile

Table 1. Bond lengths (in Å), bond angles (in degree) and dihedral angles (in degree) of the dye 1,4-Phenylenediacetonitrile

Parameters	HF/6-311G(d,p)	B3LYP/6-311G(d,p)
Bond Angle (°)		
C2-C1-C6	118.6919	118.6745
C2-C1-C8	122.745	121.6765
C6-C1-C8	118.5605	119.6007
C1-C2-C3	120.3928	120.4707
C1-C2-H13	120.0841	120.2416
C3-C2-H13	119.5231	119.2867
C2-C3-C4	120.9151	120.8548
C2-C3-H14	119.1229	119.1107
C4-C3-H14	119.9621	120.0345
C3-C4-C5	118.6922	118.6746
C3-C4-C11	118.5574	119.5974
C5-C4-C11	122.7479	121.6797
C4-C5-C6	120.3925	120.4705
C4-C5-H15	120.0804	120.2427
C6-C5-H15	119.527	119.2857
C1-C6-C5	120.9155	120.8549
C1-C6-H16	119.9588	120.0353
C5-C6-H16	119.1257	119.1098
C1-C8-C7	114.8559	113.7148

Parameters	HF/6-311G(d,p)	B3LYP/6-311G(d,p)
C1-C8-H17	109.8893	110.3802
C1-C8-H18	109.9022	110.3448
C7-C8-H17	107.7009	107.3913
C7-C8-H18	107.806	107.6276
H17-C8-H18	106.3139	107.1119
C4-C11-C10	114.8521	113.7166
C4-C11-H19	109.8987	110.3444
C4-C11-H20	109.8913	110.3797
C10-C11-H19	107.8055	107.627
C10-C11-H20	107.7017	107.3911
H19-C11-H20	106.3152	107.1117
DIHEDRAL Angle (°)		
C6-C1-C2-C3	-0.0019	-0.0568
C6-C1-C2-H13	179.8959	179.5662
C8-C1-C2-C3	179.4093	177.4052
C8-C1-C2-H13	-0.6928	-2.9718
C2-C1-C6-C5	0.0025	0.0571
C2-C1-C6-H16	-179.9973	179.9515
C8-C1-C6-C5	-179.4337	-178.4589
C8-C1-C6-H16	0.5665	0.5325
C8-C1-C8-C7	5.1783	4.9902
C2-C1-C8-H17	-116.4186	115.7707
C2-C1-C8-H18	126.9229	125.031
C6-C1-C8-C7	-175.4097	-174.5708
C6-C1-C8-H17	62.9934	63.6683

Parameters	HF/6-311G(d,p)	B3LYP/6-311G(d,p)
DIHEDRAL Angle (°)		
C6-C1-C8-H18	-53.6651	-52.53
C1-C2-C3-C4	-0.0021	0.0578
C1-C2-C3-H14	179.9942	-179.9505
H13-C2-C3-C4	-179.9006	-179.5687
H13-C2-C3-H14	0.0957	0.4229
C2-C3-C4-C5	0.0056	-0.0567
C2-C3-C4-C11	179.4589	177.4571
H14-C3-C4-C5	-179.9907	179.9819
H14-C3-C4-C11	-0.5373	-1.5345
C3-C4-C5-C6	-0.005	-0.0565
C3-C4-C5-H15	-179.9136	-179.5662
C11-C4-C5-C6	-179.4341	-179.4031
C11-C4-C5-H15	0.6573	1.9742
C3-C4-C11-C10	175.565	174.6413
C3-C4-C11-H19	53.8236	54.6003
C3-C4-C11-H20	-62.8355	-63.5973
C5-C4-C11-C10	-5.0052	-5.922
C5-C4-C11-H19	-126.7466	-146.963
C5-C4-C11-H20	116.5943	115.8394
C4-C5-C6-C1	0.001	-0.058
C4-C5-C6-H16	-179.9992	179.9506
H15-C5-C6-C1	179.9101	179.5683
H15-C5-C6-H16	-0.0901	-0.4232

Table 2. Polarizability (α) of the dye 1,4-Phenylenediacetonitrile (in a.u.).

α_{xx}	α_{xy}	α_{yy}	α_{xz}	α_{yz}	α_{zz}	α	$\Delta\alpha$
-108.40	21.28	-63.48	-1.404	0.29	-71.21	81.03	29.42

Table 3. Hyperpolarizability (β) of the dye 1,4-Phenylenediacetonitrile (in a.u.).

β_{xxx}	β_{xxy}	β_{xyy}	β_{yyy}	β_{xxz}	β_{xyz}	β_{yyz}	β_{xzz}	β_{yzz}	β_{zzz}	β_{ii}
-3.03	44.3	0.17	3.12	0.14	-0.03	0.02	0.082	0.54	0.005	0.099

Table 4. Computed excitation energies, electronic transition configurations and oscillator strengths (f) for the optical transitions with f > 0.01 of the absorption bands in visible and near- UV region for the dye 1,4-Phenylenediacetonitrile in acetonitrile

State	Configurations composition (corresponding transition orbitals)	Excitation energy (eV/nm)	oscillator strength (f)
1	-0.11422 (40 → 43) 0.66348 (42 → 43)	3.2354/383.22	0.1736
2	-0.19643 (39 → 43) 0.64433 (40 → 43)	3.6279/341.75	0.0102
3	-0.40308 (41 → 43) 0.57400 (42 → 44)	4.0847/303.53	0.0018
4	-0.13068 (39 → 44) 0.54484 (41 → 43) 0.38388 (42 → 44)	4.2965/288.57	0.0407
5	0.67671 (37 → 43)	4.6629/265.90	0.0023
6	0.62581 (39 → 43) 0.18544 (40 → 43) 0.10230 (42 → 45)	4.7976/ 258.43	0.1797
7	-0.11683 (41 → 44) 0.66930 (42 → 45)	5.3675/ 230.99	0.0056
8	0.53978 (38 → 43) -0.23462 (39 → 44) -0.21208 (40 → 44) 0.11172 (41 → 44)	5.6747/ 218.48	0.0444
9	0.17949 (38 → 43) -0.10102 (39 → 44) 0.66002 (40 → 44)	5.7753/214.68	0.0169
10	-0.25332 (39 → 44) 0.59300 (42 → 46) 0.16491 (42 → 47) 0.11605 (42 → 48)	5.8779/ 210.93	0.0079
11	-0.19934 (38 → 43) -0.27367 (39 → 44) -0.12084 (39 → 45) 0.48237 (41 → 44) -0.22193 (41 → 45) -0.12342(42 → 46)	5.8861/ 210.64	0.2558
12	0.43701 (39 → 44) 0.36097 (41 → 44) 0.18882 (41 → 45) 0.26091(42 → 46)	5.9701/ 207.67	0.3456
13	-0.14555 (42 → 46) 0.66967 (42 → 47) -0.12264 (42 → 48)	6.2555/198.20	0.0249
14	0.15520 (33 → 43) -0.30583 (34 → 43) 0.60426 (36 → 43)	6.3612/ 194.91	0.0010
15	0.13627 (35 → 43) 0.63655 (38 → 44) 0.19102 (42 → 48)	6.4833/ 191.23	0.0019
16	-0.21212 (38 → 44) -0.17297 (42 → 46) 0.60085 (42 → 48) 0.17816 (42 → 49)	6.4990/ 190.77	0.0024
17	-0.18347 (33 → 43) 0.53990 (34 → 43) 0.19248 (35 → 43) 0.34089 (36 → 43)	6.5647/188.87	0.0225
18	-0.20389 (34 → 43) 0.64141 (35 → 43) -0.11201 (38 → 44)	6.6493/186.46	0.0077
19	-0.20206 (42 → 48) 0.65829 (42 → 49)	6.7091/ 184.80	0.0083
20	0.67637 (37 → 44) -0.14058 (40 → 45)	6.7637 /183.31	0.0005

Where I_0 is the photon flux, J_{sc} is the short-circuit photocurrent density, and V_{oc} is the open-circuit photovoltage, and ff represents the fill factor [53]. At present, the J_{sc}, the V_{oc}, and the ff are only obtained by experiment, the relationship among these quantities and the electronic structure of dye is still unknown. The analytical relationship between V_{oc} and E_{LUMO} may exist. According to the sensitized mechanism (electron injected from the excited dyes to the semiconductor conduction band) and single electron and single state approximation, there is an energy relationship:

$$eV_{oc} = E_{LUMO} - E_{CB}$$

Where, E_{CB} is the energy of the semiconductor's conduction band edge. So the V_{oc} may be obtained applying the following formula:

$$V_{oc} = \frac{(E_{LUMO} - E_{CB})}{e}$$

It induces that the higher the E_{LUMO}, the larger the V_{oc}. The results of organic dye sensitizer JK16 and JK17 [39], D-ST and D-SS also proved the tendency [54] (JK16: LUMO = -2.73 eV, V_{oc} = 0.74 V; JK17: LUMO = -2.87 eV, V_{oc} = 0.67 V; D-SS: LUMO = -2.91 eV, V_{oc} = 0.70 V; D-ST: LUMO = -2.83 eV, V_{oc} = 0.73 V). Certainly, this formula expects further test by experiment and theoretical calculation. The J_{sc} is determined by two processes, one is the rate of electron injection from the excited dyes to the conduction band of semiconductor, and the other is the rate of redox between the excited dyes and electrolyte. Electrolyte effect on the redox processes is very complex, and it is not taken into account in the present calculations. This indicates that most of excited states of 1,4-Phenylenediacetonitrile have larger absorption coefficient, and then with shorter lifetime for the excited states, so it results in the higher electron injection rate which leads to the larger J_{sc} of 1,4-Phenylenediacetonitrile. On the basis of above analysis, it is clear that the 1,4-Phenylenediacetonitrile has better performance in DSSC.

Conclusion

The geometries, electronic structures, polarizabilities, and hyperpolarizabilities of dye 1,4-Phenylenediacetonitrile was studied by using ab initio HF and density functional theory with hybrid functional B3LYP, and the UV-Vis spectra were investigated by using TD-DFT methods. The NBO results suggest that 1,4-Phenylenediacetonitrile is a (D-p-A) system. The calculated isotropic polarizability of 1,4-Phenylenediacetonitrile is 81.03 a.u. The calculated polarizability anisotropy invariant of 1,4-Phenylenediacetonitrile is 29.42 a.u and its hyperpolarizability of 1,4-Phenylenediacetonitrile is 0.099 a.u.. The electronic absorption spectral features in visible and near-UV region were assigned based on the qualitative agreement to TD-DFT calculations. The absorptions are all ascribed to $\pi \rightarrow \pi^*$ transition. The three excited states with the lowest excited energies of 1,4-Phenylenediacetonitrile is photoinduced electron transfer processes that contributes sensitization of photo-to-current conversion processes. The interfacial electron transfer between semiconductor TiO_2 electrode and dye sensitizer 1,4-Phenylenediacetonitrile is electron injection process from excited dye as donor to the semiconductor conduction band. Based on the analysis of geometries, electronic structures, and spectrum properties between 1,4-Phenylenediacetonitrile the role of nitro group is as follows: it enlarged the distance between electron donor group and semiconductor surface, and decreased the timescale of the electron injection rate, resulted in giving lower conversion efficiency. This indicates that the choice of the appropriate conjugate bridge in dye sensitizer is very important to improve the performance of DSSC.

References:

[1] B. Li, L. Wang, B. Kang, P. Wang, Y. Qiu, Sol. Energy Mater. Sol. Cells 90 (2006) 549.
[2] B. O'Regan, M. Gratzel, Nature 353 (1991) 737.
[3] M. Gratzel, J. Photochem. Photobiol. C 4 (2003) 145.
[4] M. Gratzel, J. Photochem. Photobiol. A 164 (2004) 3.
[5] M.K. Nazeeruddin, C. Klein, P. Liska, M. Gratzel, Coord. Chem. Rev. 249 (2005) 1460.
[6] T. Dittrich, B. Neumann, H. Tributsch, J. Phys. Chem. C 111 (2007) 2265.
[7] X.Z. Liu, Y.H. Luo, H. Li, Y.Z. Fan, Z.X. Yu, Y. Lin, L.Q. Chen, Q.B. Meng, Chem. Commun. 27 (2007) 2847.
[8] J.B. Xia, F.Y. Li, H. Yang, X.H. Li, C.H. Huang, J. Mater. Sci. 42 (2007) 6412.
[9] M.X. Li, X.B. Zhou, H. Xia, H.X. Zhang, Q.J. Pan, T. Liu, H.G. Fu, C.C. Sun, Inorg. Chem. 47 (2008) 2312.
[10] E. Muller, P. Liska, N. Vlachopoulos, M. Gratzel, J. Am. Chem. Soc. 115 (1993) 6382.
[11] M.K. Nazeeruddin, P. Pechy, T. Renouard, S.M. Zakeeruddin, R. Humphry-Baker, P. Comte, P. Liska, L. Cevey, E. Costa, V. Shklover, L. Spiccia, G.B. Deacon, C.A. Bignozzi, M. Gratzel, J. Am. Chem. Soc. 123 (2001) 1613.
[12] M. Gratzel, Inorg. Chem. 44 (2005) 6841.
[13] K. Hara, T. Sato, R. Katoh, A. Furube, Y. Ohga, A. Shinpo, S. Suga, K. Sayama, H.Sugihara, H. Arakawa, J. Phys. Chem. B 107 (2003) 597.
[14] X.H. Zhang, C. Li, W.B. Wang, X.X. Cheng, X.S. Wang, B.W. Zhang, J. Mater. Chem. 17 (2007) 642 (and reference therein).
[15] M. Liang, W. Xu, F. Cai, P. Chen, B. Peng, J. Chen, Z. Li, J. Phys. Chem. C 111 (2007) 4465 (and reference therein).
[16] W. Xu, B. Peng, J. Chen, M. Liang, F. Cai, J. Phys. Chem. C 112 (2008) 874.
[17] F. De Angelis, S. Fantacci, A. Selloni, Chem. Phys. Lett. 389 (2004) 204.
[18] F. De Angelis, S. Fantacci, A. Selloni, M.K. Nazeeruddin, Chem. Phys. Lett.415(2005)115.
[19] Y. Xu, W.K. Chen, M.J. Cao, S.H. Liu, J.Q. Li, A.I. Philippopoulos, P. Falaras, Chem. Phys. 330 (2006) 204.
[20] M.K. Nazeeruddin, F. De Angelis, S. Fantacci, A. Selloni, G. Viscardi, P. Liska, S. Ito, B. Takeru, M. Gratzel, J. Am. Chem. Soc. 127 (2005) 16835.
[21] F. De Angelis, S. Fantacci, A. Selloni, M. Gratzel, M.K. Nazeeruddin, Nano. Lett. 10 (2007) 3189.
[22] F. De Angelis, S. Fantacci, A. Selloni, M.K. Nazeeruddin, M. Gratzel, J. Am. Chem. Soc. 129 (2007) 14156.
[23] F. De Angelis, S. Fantacci, A. Selloni, Nanotechnology 19 (2008) 424002.
[24] D. Di Censo, S. Fantacci, F. De Angelis, C. Klein, N. Evans, K. Kalyanasundaram, H.J. Bolink, M. Gratzel, M.K. Nazeeruddin, Inorg. Chem. 47 (2008) 980.
[25] Y. Kurashige, T. Nakajima, S. Kurashige, K. Hirao, Y. Nishikitani, J. Phys. Chem. A 111 (2007) 5544.
[26] M.P. Balanay, D.H. Kim, Phys. Chem. Chem. Phys. 10 (2008) 5121.
[27] P. Persson, M.J. Lundqvist, J. Phys. Chem. B 109 (2005) 11918.

[28] P. Persson, M.J. Lundqvist, R. Ernstorfer, W.A. Goddard III, F. Willig, J. Chem. Theory Comput. 2 (2006) 441.

[29] M.J. Lundqvist, M. Nisling, S. Lunell, B. Akermark, P. Persson, J. Phys. Chem. B 110 (2006) 20513.

[30] M. Nilsing, P. Persson, S. Lunell, L. Ojamae, J. Phys. Chem. C 111 (2007) 12116.

[31] W.R. Duncan, O.V. Prezhdo, Annu. Rev. Phys. Chem. 58 (2007) 143.

[32] W.R. Duncan, O.V. Prezhdo, J. Am. Chem. Soc. 130 (2008) 9756.

[33] L.G.C. Rego, V.S. Batista, J. Am. Chem. Soc. 125 (2003) 7989.

[34] Z.Y. Guo, Y. Zhao, W.Z. Liang, G.H. Chen, J. Phys. Chem. C 112 (2008) 16655.

[35] I. Kondov, M. Clzek, C. Benesch, H.B. Wang, M. Thoss, J. Phys. Chem. C 111 (2007) 11970.

[36] N. Robertson, Angew. Chem. Int. Ed. 45 (2006) 2338.

[37] S. Ito, H. Miura, S. Uchida, M. Takata, K. Sumioka, P. Liska, P. Comte, P. Pechy, M. Gratzel, Chem. Commun. (2008), 5194-5196.

[38] M.J. Frisch, G.W. Trucks, H.B. Schlegel, G.E. Scuseria, M.A. Robb, J.R. Cheeseman, J.A.Montgomery Jr., T. Vreven, K.N. Kudin, J.C. Burant, J.M. Millam, S.S. Iyengar, J. Tomasi, V. Barone, B. Mennucci, M. Cossi, G. Scalmani, N. Rega, G.A. Petersson, H. Nakatsuji, M.Hada, M. Ehara, K. Toyota, R. Fukuda, J. Hasegawa, M. Ishida, T. Nakajima, Y. Honda, O. Kitao, H. Nakai, M. Klene, X. Li, J.E. Knox, H.P. Hratchian, J.B. Cross, C. Adamo, J. Jaramillo, R. Gomperts, R.E. Stratmann, O. Yazyev, A.J. Austin, R. Cammi, C. Pomelli, J.W. Ochterski, P.Y. Ayala, K. Morokuma, G.A. Voth, P. Salvador, J.J. Dannenberg, V.G.Zakrzewski, S.Dapprich, A.D. Daniels, M.C. Strain, O. Farkas, D.K. Malick, A.D. Rabuck, K. Raghavachari, J.B. Foresman, J.V. Ortiz, Q. Cui, A.G. Baboul, S. Clifford, J.Cioslowski, B.B. Stefanov, G. Liu, A. Liashenko, P. Piskorz, I. Komaromi, R.L. Martin, D.J. Fox, T. Keith, M.A.Al-Laham, C.Y. Peng, A. Nanayakkara, M. Challacombe, P.M.W. Gill, B. Johnson, W. Chen, M.W. Wong, C. Gonzalez, J.A. Pople, Gaussian 03, Gaussian, Inc., Pittsburgh, PA, 2003.

[39] A.D. Becke, J. Chem. Phys. **98** (1993), 5648-5652.

[40] B. Miehlich, A. Savin, H. Stoll, H. Preuss, Chem. Phys. Lett. **157** (1989), 200-206.

[41] C. Lee, W. Yang, R.G. Parr, Phys. Rev. B. **37** (1988), 785-789.

[42] V. Barone, M. Cossi, J. Phys. Chem. A **102** (1998), 1995-2001.

[43] M. Cossi, N. Rega, G. Scalmani, V. Barone, J. Comput. Chem. **24** (2003), 669-681.

[44] M.K. Nazeeruddin, F. De Angelis, S. Fantacci, A. Selloni, G. Viscardi, P. Liska, S.Ito, B. Takeru, M. Gratzel, J. Am. Chem. Soc. **127** (2005), 16835-16847.

[45] M.J. Lundqvist, M. Nilsing, P. Persson, S. Lunell, Int. J. Quantum Chem. **106** (2006), 3214 3234

[46] D.F. Waston, G.J. Meyer, Annu. Rev. Phys. Chem. **56** (2005), 119-156.

[47] C. R. Zhang, H. S. Chen, and G. H. Wang, Chem. Res. Chin. U. **20** (2004), 640-646.

[48] Y. Sun, X. Chen, L. Sun, X. Guo, W. Lu, Chem.Phys. Lett. **381** (2003), 397-403.

[49] O. Christiansen, J. Gauss, J. F. Stanton, Chem.Phys. Lett. **305** (1999), 147-155.

[50] Z. S. Wang, Y. Y. Huang, C. H. Huang, J. Zheng, H.M. Cheng, S. J. Tian, Synth. Met. **14** (2000), 201-207.

[51] C.R. Zhang, Y.Z. Wu, Y.H. Chen, H.S. Chen, Acta Phys. Chim. Sin. **25** (2009), 53-60.

[52] A. Seidl, A. Gorling, P. Vogl, J. A. Majewski, M. Levy, Phys. Rev. B **53** (1996), 3764 3774.

[53] K. Hara, T. Sato, R. Katoh, A. Furube, Y. Ohga, A. Shinpo, S. Suga, K. Sayama, H.Sugihara, H. Arakawa, J. Phys. Chem. B. **107** (2003), 597-606.

[54] C.R. Zhang, Z.J. Liu, Y.H. Chen, H.S. Chen, Y.Z. Wu, L.H. Yuan, J. Mol. Struct.(THEOCHEM) **899** (2009), 86-93.